

## Determination of the dust screening length by laser-excited lattice waves

A. Homann, A. Melzer, S. Peters, and A. Piel

*Institut für Experimentalphysik, Christian-Albrechts-Universität Kiel, D-24098 Kiel, Germany*

(Received 16 April 1997)

The screening of dust particles immersed in the sheath of a parallel plate rf discharge in helium is studied by excitation of waves in a linear chain arrangement. The waves are excited by the radiation pressure of a modulated laser beam. The measured dispersion relation is compared with a one-dimensional dust lattice wave to obtain the shielding length. Dust acoustic waves are not compatible with the measured dispersion relation. [S1063-651X(97)11611-7]

PACS number(s): 52.35.Fp, 52.25.Vy

### I. INTRODUCTION

Since the first experimental observation in 1994 [1–3], the plasma crystal has attracted a growing interest from the astrophysics, plasma technology, and condensed matter communities. The crystal can serve as a model system to investigate structures and dynamics as well as the solid-liquid phase transition in an intermediate state between two and three dimensions.

In a rf plasma, micrometer-sized dust particles typically acquire a negative charge of several thousand elementary charges and are trapped in the lower sheath of the discharge by an inwardly directed electric field force. The particles interact with each other through their strong Coulomb repulsion. As soon as the electrostatic energy of neighboring particles strongly exceeds the thermal energy, the particles arrange themselves in regular, solidlike structures. Under certain conditions this plasma crystal undergoes a phase transition from the solid to an almost gaslike state [4,5].

The mutual Coulomb repulsion of the dust grains is partly screened by the polarization of the surrounding plasma particles, mostly by ions which represent the major species in the sheath. Therefore knowledge of the charge on the particles and the screening length is of central interest, in particular for a quantitative comparison with theoretical phase diagrams. The complexity of a rf discharge sheath caused by the supersonic flow of the ions and the non-neutrality conditions prevent us from determining the shielding length from standard models. Peters *et al.* [6] have carried out experiments to determine the shielding length which are based on the electrical excitation of eigenmodes in a linear chain arrangement of dust particles. This idea is extended here to measure the complete dispersion relation of a chain of particles. In our experiment the chain is excited by a modulated laser beam instead of using an exciter wire and applying a sine voltage. In this way perturbations of the confining potential well, in which the dust grains are trapped, are avoided.

In the literature there exist two competing models to describe very-low-frequency waves in dusty plasmas: the dust lattice wave (DLW) (see, for example, [7]) and the dust acoustic wave (DAW) [8]. In a DLW the dust grains are strongly coupled and interact directly through their (shielded) Coulomb repulsion, whereas a DAW is similar to an ordinary ion acoustic wave, but where the ions provide the pressure and the grains the inertia.

Here we present investigations of laser-excited waves in a

linear chain arrangement, which aim at measuring the dispersion relation and from this determine the ion Debye length in the sheath of a rf discharge. The linear chain serves as a simple model for a whole dust crystal [7] and has the advantage to be treatable with one-dimensional (1D) models. The experimental data are compared with the dispersion relations of the DLW and DAW.

### II. DLW AND DAW

For comparison with the theory of the DLW an infinite linear chain arrangement of equal masses  $m$  has to be considered. For the equation of motion one finds

$$m\ddot{\xi}^{(n)} + m\beta\dot{\xi}^{(n)} = \sum_{l=-\infty}^{+\infty} F_l^{(n)}, \quad (1)$$

where  $\xi^{(n)}$  is a small elongation of the  $n$ th particle from its equilibrium position,  $\beta$  is the Epstein friction [9], and  $\sum F_l^{(n)}$  describes the Coulomb interaction between the  $n$ th and the  $l$ th particle.

Here the grains are assumed to interact through a screened Coulomb potential:

$$\phi = \frac{Q}{4\pi\epsilon_0 a} \exp\left(-\frac{a}{\lambda_D}\right). \quad (2)$$

$Q$  is the bare charge of the particles,  $a$  the next-neighbor distance, and  $\lambda = a/\lambda_D$  describes the screening strength, with  $\lambda_D$  being the shielding length. It should be mentioned that  $\lambda_D$ , which is measured in our experiment, is not the thermal ion Debye length in a plasma, but that for the special conditions in a rf sheath with non-neutrality and the supersonic flow of the ions. With the usual ansatz for waves on a linear chain,  $\xi^{(n)} = \xi_0 \exp[i(nqa - \omega t)]$ , the dispersion relation of a DLW reads (see, for example, [7]):

$$\omega^2 + i\beta\omega - 4 \sum_{l=1}^N \gamma_l \sin^2\left(\frac{lqa}{2}\right) = 0, \quad (3)$$

with

$$\gamma_l = \frac{Q^2}{2\pi\epsilon_0 m (la)^3} \exp(-l\lambda) \left(1 + l\lambda + \frac{(l\lambda)^2}{2}\right). \quad (4)$$

Here  $q = q_r + iq_i$  denotes the complex wave number,  $\omega$  being real in a driven system. The index  $N$  indicates the number of interacting particles; e.g.,  $N=1$  includes next-neighbor interactions only, and  $N=2$  also includes that of overnext neigh-

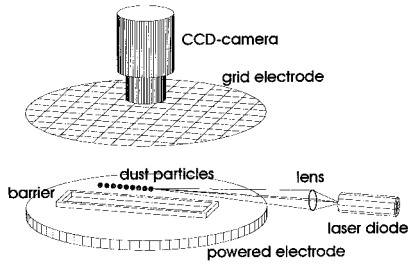


FIG. 1. The experimental setup.

bors. For  $\lambda$  of the order of 1 it is sufficient to consider next- and overnext-neighbor interactions ( $N=2$ ) as pointed out by Melandsø [7]. The DLW is based on strong Coulomb interactions between the dust particles; i.e., the system is strongly coupled.

In contrast, dust acoustic waves assume a weak-coupling approximation. This wave mode was first predicted theoretically by Rao *et al.* [8] yielding the dispersion relation (we use here the expression in [10] where the authors have added a drag term)

$$q^2 = \frac{1}{\lambda_D^2} \frac{\omega(\omega + i\beta)}{\omega_d^2 - \omega(\omega + i\beta)}, \quad (5)$$

where  $\omega_d^2 = (Q^2 n_d) / (\epsilon_0 m)$  is the dust plasma frequency with the dust number density  $n_d^{-1} = (4\pi a^3)/3$ . Here  $\lambda_D$  also considers the conditions in the rf sheath. The particles' interactions in this mode are indirect: The dust particles provoke ion density fluctuations which in turn influence the particles. Dust acoustic waves have been observed in several experiments. The DAW can be self-excited [11] or excited by sinusoidal voltages on a wire probe [10].

### III. EXPERIMENTAL METHOD

The experimental setup is similar to that used in [6]. The dust particles are trapped in the lower sheath of a parallel plate rf discharge operated in helium. The upper electrode is grounded and the lower one is powered at a frequency of 13.56 MHz and a rf power of 7 W. In order to arrange the dust grains in a linear chain a rectangular barrier of  $z=4$  mm height and  $x=90$  mm  $\times$   $y=20$  mm inner spacing is put on the lower electrode (see Fig. 1).

In the measurement described here we inserted 12 monodisperse spherical melamine formaldehyde (MF) plastic particles of  $d=(9.5 \pm 0.3)$   $\mu\text{m}$  diameter and a mass density of  $\rho=1514$   $\text{kg/m}^3$  into the plasma chamber. These particles arrange in a linear chain with an interparticle distance of  $a=930$   $\mu\text{m}$  at a gas pressure of 22 Pa. For observation the particles are illuminated by a horizontally expanded thin laser sheet. The whole arrangement is viewed in scattered light from the top with a video camera, and the images are stored on a tape recorder.

The beam (20 mW, 690 nm) of a laser diode is focused on the first particle. The laser's radiation pressure pushes the first particle, thus exciting the chain. Although the focus diameter is larger than the particle diameter, the particle must be close to the inner focus to be moved by the laser. The other particles are in the defocused region and are therefore

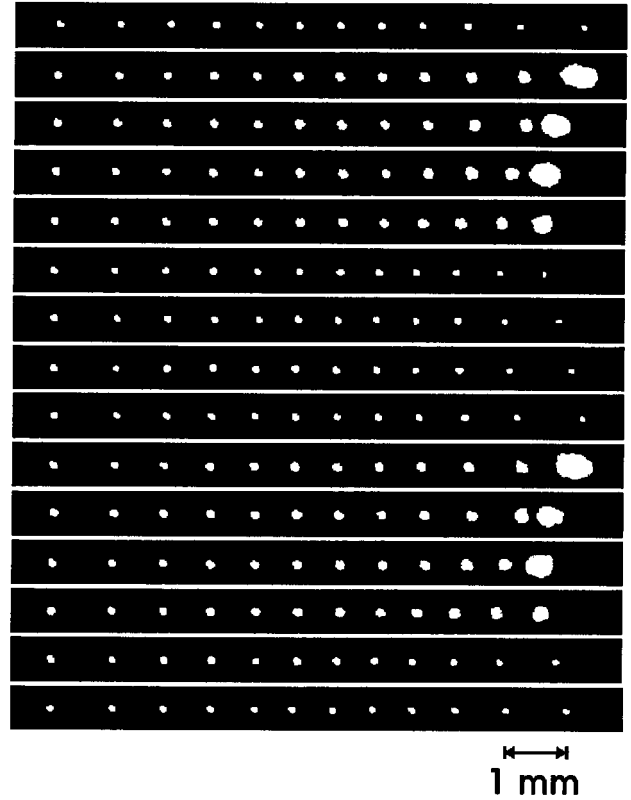


FIG. 2. Sequence of 15 snapshots for a linear chain arrangement of 12 particles. The time step between each image is 100 ms. It is clearly seen that only the first particle is pushed by the exciting laser.

nearly unaffected by the beam. The laser diode is switched on and off by a transistor-transistor-logic (TTL) signal. In our experiment the switching frequency  $f$  was varied between 0.4 Hz and 3 Hz with a constant duty cycle of 50%. Above 3 Hz the motion of the dust particles is too small for observation.

The mechanism of the excitation is mainly attributed to radiation pressure. It is well known that small particles can be accelerated by a laser beam to several times the acceleration of gravity [12]. For our 20 mW laser the force is of the order of, or smaller than, the gravitational force. Thermophoretic forces due to an inhomogeneous absorption of the laser energy resulting in a temperature gradient across the particle can be neglected [13]. The characteristic time for heat conduction within the particle  $\tau \approx (d/2)^2 / \kappa$  with a thermal diffusivity  $\kappa \approx 2 \times 10^{-7}$   $\text{m}^2/\text{s}$  for the MF dust yields  $\tau < 1$  ms, which is much shorter than the laser pulse ( $\tau_L > 100$  ms). Hence it can be concluded that the temperature profile within the particle is uniform. Furthermore, this effect would cause a backwards motion with respect to the laser beam (negative photophoresis), which is in contrast to the observations. Evaporation can also be neglected because of the rather low laser intensity and the thermal stability of the MF dust up to 600 K.

### IV. RESULTS AND DISCUSSION

Because of the narrow width of the potential well in the  $y$  direction (due to the barrier) and  $z$  direction (due to the balance of gravitational force and electrostatic field force), the

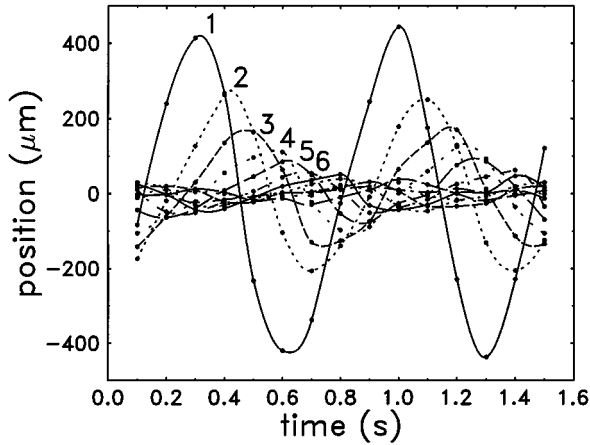


FIG. 3. The oscillatory motion of the 12 particles relative to their individual equilibrium positions at 1.3 Hz. The curves of the first 6 particles are indicated, where “1” corresponds to the excited particle. The other particle trajectories are not labeled for clarity.

particles can only move in the  $x$  direction. Figure 2 gives an impression of their oscillatory motion. It shows a series of video images at a frequency of 1.3 Hz and at a pressure of 22 Pa. The time step between each video image is 100 ms. Only the rightmost dust particle is forced by the laser beam which can be clearly seen by the bright spot of scattered light in these images. Note that the exciting laser is “on” in images 2–5 and 10–13. In the other images the laser is “off.”

The analysis of the video sequences is performed in the usual way [6]. The trajectory of each particle is followed through several frames. The motion is then separated into a time-averaged position and into an elongation about this equilibrium, yielding the oscillation amplitudes and phases of each dust grain. In Fig. 3 one can see the oscillatory part of the particles motion about their individual equilibrium positions. Although the applied force to the first particle is a square wave, the motion of all the particles turns out as almost sinusoidal. The rather large amplitude of the first particle, especially for low frequencies, may require a nonlinear treatment. However, its nonlinearity is negligible since for the extraction of the wavelength all particles are considered. Furthermore, we have omitted the first particle from the analysis of the damping length. The phases and the oscillation amplitudes as a function of the particle position (the rightmost particle is the excited) are shown for four different frequencies in Fig. 4. It should be noticed that at 1 Hz one full wavelength is excited in the linear chain arrangement [Fig. 4(a)]. The oscillation amplitudes of the particles decrease exponentially over distance with a damping length of 4.3 (2.1) interparticle distances at 0.5 Hz (3 Hz) [Fig. 4(b)]. The linear phase shift and the exponential decaying amplitudes give the wavelength and the damping length, respectively, which correspond to the real ( $q_r$ ) and imaginary part ( $q_i$ ) of the wave number  $q$ .

In this way we have measured the dispersion relation for a 12-particle chain at 22 Pa and 7 W, shown in Fig. 5, denoted by symbols. The interaction of the particles with each other, i.e., the dispersion relation, contains the information of the shielded charge.

The bare, unshielded charge  $Q$  of the dust particles is measured from vertical particle oscillations with the usual

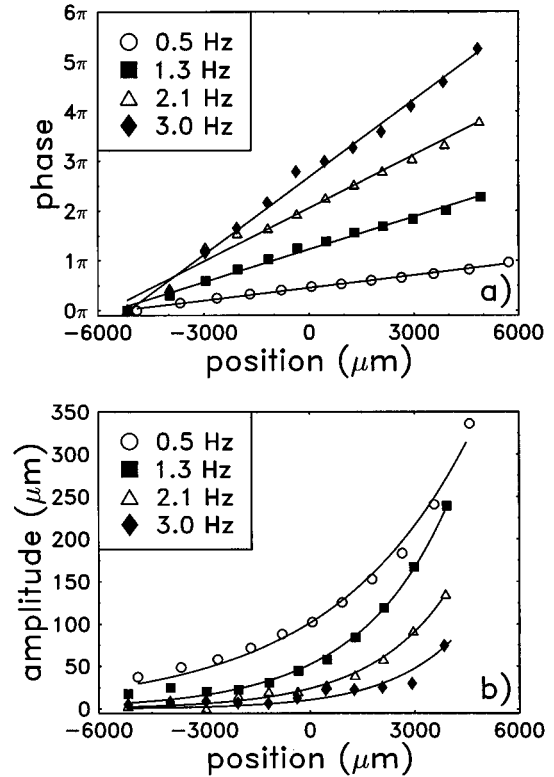


FIG. 4. Phase shift (a) and wave damping (b) of the particles for four different frequencies.

resonance method [3,14]. For the chosen pressure of 22 Pa and a power of 7 W, we obtain  $Q = 14\,000e$  with an uncertainty  $\Delta Q = +4000e$  due to the influence of the electrons during a rf cycle [14].

Let us first consider the DLW: The real and imaginary parts of Eq. (3) are compared with our experimental data for different shielding strength  $\lambda$ . The friction in that system due to neutral gas drag is calculated from the Epstein formula [9] as  $\beta = (6.3-9.1) \text{ s}^{-1}$  for 22 Pa depending on the Millikan coefficient. From our resonance curves for vertical oscillations, used for measuring the unshielded particle charges, we obtain values for  $\beta$  that are slightly larger than the upper Epstein limit. With the constant particle charge of  $Q = 14\,000e$  and a friction term varying between  $6 \text{ s}^{-1}$  and  $12 \text{ s}^{-1}$ , the screening length  $\lambda_D$  was fitted simultaneously to the real and imaginary branches of the dispersion relation. From the fit  $\beta = (9.5 \pm 1) \text{ s}^{-1}$  and  $\lambda = a/\lambda_D = (1.1 \pm 0.1)$  are obtained. In Fig. 5 (solid line) the dispersion relation of a DLW for these parameters are shown together with the experimental data. A very close agreement between these two curves and the measured points is found, indicating that the investigated oscillations can be described by the DLW model.

For the maximum expected particle charge of  $Q = 18\,000e$ , a screening strength of  $\lambda = 2.2$  results. Thus, a screening strength of  $\lambda = (1.6 \pm 0.6)$  can be derived from the experiment. This is in fair agreement with the measured screening strength of  $\lambda = 1.5-2$  in [6] and with  $\lambda = 1$  as proposed in Ref. [15].

For comparison, we have additionally plotted in Fig. 5 the dispersion relation of a DAW [see Eq. (5)] for two different sets of parameters. The dotted curve is obtained by using the

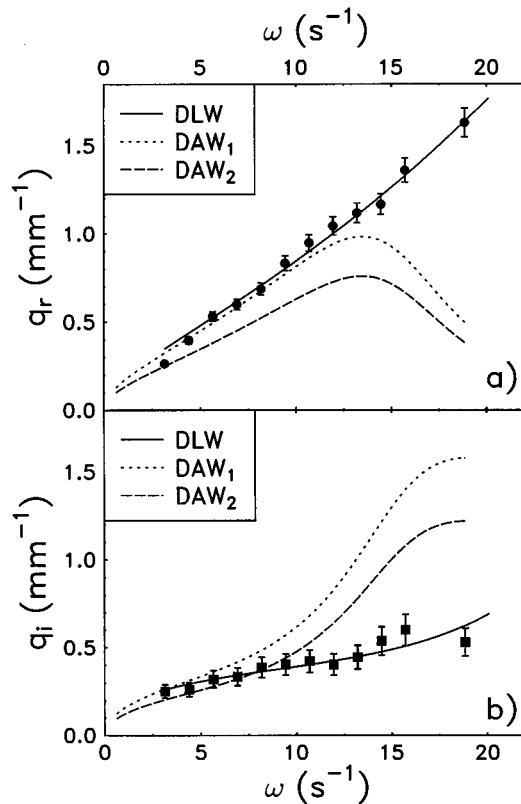


FIG. 5. Measured dispersion relation denoted by symbols and the theoretical dispersion relation of a DLW (solid line) and a DAW (dotted and dashed lines) are shown. For the DAW two sets of parameters are plotted. Dotted line: same parameters as DLW. Dashed line: best fit for  $\lambda$ . For details see text. In (a) the real parts and in (b) the imaginary parts are shown. The DLW model represents very well the experimental points, whereas the DAW model is not in agreement with the experimental data.

same parameters as for the DLW ( $Q = 14\,000e$ ,  $\beta = 9.5 \text{ s}^{-1}$ ,  $\lambda = 1.1$ ). For  $\omega < 10 \text{ s}^{-1}$  the real branches [Fig. 5(a)] of the DAW and the DLW are almost identical and fit the data well. For  $\omega > 10 \text{ s}^{-1}$ , however, the DAW and the experimental data have an opposite behavior: The DAW curve decisively decreases in contrast to the data. The imaginary branch of the DAW [Fig. 5(b)] is always above the measured points. Es-

pecially for  $\omega > 10 \text{ s}^{-1}$  strong deviations occur.

The dashed curve in Fig. 5 is the result of a simultaneous fit of the screening strength  $\lambda$  to the real and imaginary parts of the dispersion relation for the measured charge of  $Q = 14\,000e$  and  $\beta = 9.5 \text{ s}^{-1}$ , yielding  $\lambda = 0.8$ . For these parameters the real branch is always below the measured data points. This fit also shows severe deviations from the experiment. For a particle charge of  $Q = 18\,000e$  the fits are slightly better, but still do not agree with the experimental data.

Different from our findings, Pieper and Goree [10] observed dust-acoustic-wave-type particle motions in a strongly coupled system. In their experiments which were performed under comparable conditions, plane waves were launched in a horizontally extended plasma crystal by a wire probe. The resulting dispersion relations could be described by a DAW model.

Summarizing, the DLW model is much more appropriate to represent our experimental data. The interaction of the particles can therefore be attributed to a strong (shielded) Coulomb repulsion. The coupling parameter  $\Gamma = Q^2 / (4\pi\epsilon_0 akT)$ , which describes the ratio of the electrostatic energy of neighboring particles and the thermal energy, is calculated to  $\Gamma = 10\,000$  for the investigated system. This high value of  $\Gamma$  supports the finding of strongly coupled dust lattice waves.

## V. CONCLUSIONS

In conclusion we have determined the shielding strength by wave excitation in a strongly coupled linear particle arrangement. The excitation of the dust arrangement by a focused diode laser beam turned out to be a suitable novel technique. The shielding strength in that system is found to be  $\lambda = (1.6 \pm 0.6)$  which is in fair agreement with former investigations. The measured dispersion relation can be described by dust lattice waves with very close agreement. Dust acoustic waves, however, disagree with the dispersion relation.

## ACKNOWLEDGMENTS

We thank J. E. Allen for a useful hint on the role of radiation pressure. This work was supported by the DFG (Grant No. Pi185/8-1).

[1] J. H. Chu and L. I, Phys. Rev. Lett. **72**, 4009 (1994).  
 [2] H. Thomas, G. E. Morfill, V. Demmel, J. Goree, B. Feuerbacher, and D. Möhlmann, Phys. Rev. Lett. **73**, 652 (1994).  
 [3] A. Melzer, T. Trottenberg, and A. Piel, Phys. Lett. A **191**, 301 (1994).  
 [4] A. Melzer, A. Homann, and A. Piel, Phys. Rev. E **53**, 2757 (1996).  
 [5] H. Thomas and G. E. Morfill, Nature (London) **379**, 806 (1996).  
 [6] S. Peters, A. Homann, A. Melzer, and A. Piel, Phys. Lett. A **223**, 389 (1996).  
 [7] F. Melandsø, Phys. Plasmas **3**, 3890 (1996).

[8] N. N. Rao, P. K. Shukla, and M. Y. Yu, Planet. Space Sci. **38**, 543 (1990).  
 [9] P. S. Epstein, Phys. Rev. **23**, 710 (1924).  
 [10] J. B. Pieper and J. Goree, Phys. Rev. Lett. **77**, 3137 (1996).  
 [11] A. Barkan, R. L. Merlino, and N. D'Angelo, Phys. Plasmas **2**, 3563 (1995).  
 [12] A. Ashkin, Phys. Rev. Lett. **24**, 156 (1970).  
 [13] E. Stoffels, W. W. Stoffels, D. Vender, G. M. W. Kroesen, and F. J. de Hoog, IEEE Trans. Plasma Sci. **22**, 116 (1994).  
 [14] T. Trottenberg, A. Melzer, and A. Piel, Plasma Sources Sci. Technol. **4**, 450 (1995).  
 [15] S. V. Vladimirov and O. Ishihara, Phys. Plasmas **3**, 444 (1996).